Aspheric surface measurement based on sub-aperture stitching interferometry

Xiaokun Wang (王孝坤)

Key Laboratory of Optical System Advanced Manufacturing Technology, Changchun Institute of Optics, Fine Mechanics and Physics, Chinese Academy of Sciences, Changchun 130033, China

**Corresponding author: jimwxk@sohu.com*

Received January 19, 2013; accepted March 5, 2013; posted online July 17, 2013

In order to test convex aspheric surfaces without the aid of other null optics, a novel method combined sub-aperture stitching and interferometry called SSI (sub-aperture stitching interferometry) is introduced. In this letter, the theory, basic principle, and flow chart of SSI are researched. A synthetical optimization stitching mode and an effective stitching algorithm are established based on homogeneous coordinate's transformation and simultaneous least-squares fitting. The software of SSI is devised, and the prototype for testing of large aspheres by SSI is designed and developed. The experiment is carried out with five sub-apertures for a convex silicon carbide (SIC) aspheric mirror with a clear aperture of 130 mm. The peak-to-valley (PV) and root-mean-square (RMS) error are 0.186 λ and 0.019 λ, respectively. For the comparison and validation, the TMA system which contained the convex asphere is tested by interferometry. The wavefront error of the central field of the optical system is 0.068 λ RMS which approaches to diffraction limitation. The results conclude that this technique is feasible and accurate. It enables the non-null testing of aspheric surfaces especially for convex aspheres.

OCIS codes: 120.6650, 120.0120, 240.0240.

doi: 10.3788/COL201311.S21201.

Aspheric surfaces have great ability on correcting aberrations, improving image quality and reducing the size and weight of the system[1,2]. So they are extremely important in optical systems and have been applied in various kinds of fields. As the use of aspheres in optical systems becomes more and more prevalent, the need for precise and efficient metrology grows. One of the most promising measurements is interferometry. Because of its high resolution, high sensitivity and reproducibility, this technology has become the standard tool for testing optical surfaces and wavefronts. However, when testing the aspheric surfaces with large aperture, steep and large departure, many interference fringes are formed on the detection device and proper analysis are difficult to perform, so we will fall back on auxiliary optics such as null corrector or computer generated hologram (CGH). The auxiliary elements must have been specially designed and customized which costs much more time and cost. What is more it brings other errors including both manufacturing errors and some unavoidable misalignment errors. The cost of making and verifying the null elements conspires to keep aspheres away from practical optical designs.

Sub-aperture stitching interferometry (SSI) can expand both the longitudinal and lateral dynamic ranges of the interferometer itself, and broaden the scope of measurement significantly[3−6]. The basic idea of sub-aperture testing method was first proposed by Kim in 1982[7]. It can test large optical system by an array of smaller optical flats without large reference flat, which substantially reduces the cost and complexity. The second milestone is the discrete phase method developed by Stuhlinger[8]. Then the least-squares method to fit the relative piston and tilt by the datum of overlapping regions was introduced by Otsubo *et al.*[4,9]. The mentioned stitching methods are effective for testing large flats, but they cannot be used to measure large spheres or aspheric surfaces.

The last significant progress of SSI is the automated subaperture stitching interferometer workstation produced by QED(Queues Enforth Development, Inc.) Technologies[10−12]. It is applicable not only to plano optics, but also to spherical and moderate aspheric surfaces with the aperture smaller than 200 mm. But the mathematic model and stitching algorithm have not been described in detail by QED.

Recently we have proposed a synthetical optimization stitching algorithm for testing large aspheric surfaces by SSI[13,14]. In this letter, a prototype for testing of large aspheres with the stitching method is developed. We fabricate a convex silicon carbide (SIC) mirror by computer controlled optical surfacing (CCOS) and measured it by SSI. It shows that SSI can be used to test asphere especially for convex asphere at high resolution, low cost, and high efficiency without any null optics.

The sketch of setup for testing convex asphere by SSI is shown in Fig. 1, and the elaborate flow chart is given in Fig. 2. Firstly, we define the surface to be measured, in particular its nominal aperture and radius of the curvature. The proper transmission sphere is selected correctly, and then the size and number of the sub-aperture are determined by the surface diameter and the relative aperture[15]. The second step is to control the interferometer and the tested asphere precisely. The first null is located at the center of the surface and the curvature of the spherical wavefront is consistent with the measured region. The phase distribution of this region will be recorded. Next, when we align the interferometer or the asphere again and again, let the slope of the spherical wavefront

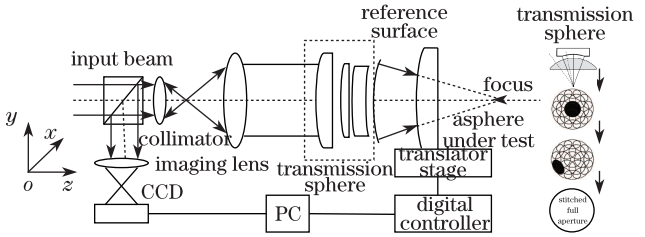

Fig. 1. (Color online) Sketch of setup for testing asphere by SSI. PC: personal computer.

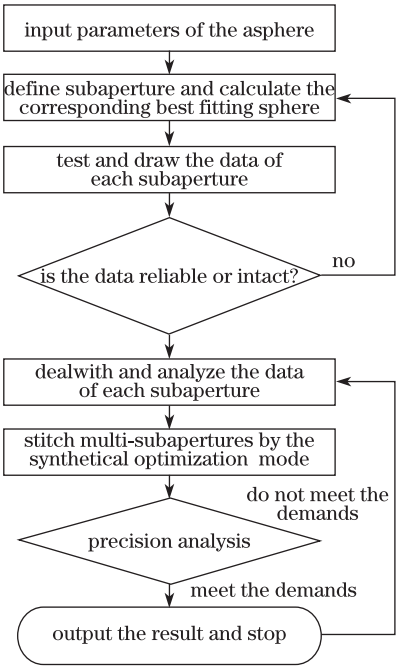

Fig. 2. (Color online) Flow chart of SSI.

match the slope of the outer sub-aperture and make sure there are some overlapping areas between the adjacent sub-apertures. Then the phase data of each subaperture is acquired by interferometric method, and the datum of the corresponding subaperture is recorded. Fourthly, we choose the subaperture in the center region of the aspheric surface as the fiducial sub-aperture and the data of all the subapertures are unified into the same reference by homogeneous coordinate's transformation. The relative translation errors are eliminated from each subaperture through the simultaneous least-squares method by minimizing the discrepancy in the overlapping areas. After all the translation errors are subtracted, a final least-squares fitting is performed to evaluate the misalignment errors of the whole system.

The phase datum of each subaperture can be obtained by interferometry, and then the data of all the subapertures can be unified into the same reference by homogeneous coordinate's transformation. We can stitch two sub-apertures by subtracting the relative translation errors of adjacent subapertures. Using the principle of two sub-apertures splicing many times may realize multi-subaperture stitching. But it often brings the erroneous transmission and accumulation, thus the precision is reduced. In this letter, the sum of the squared differences for all common areas are minimized simultaneously.

Suppose there are M sub-apertures in total. To be simple for the localization and measurement, generally choose the sub-aperture in the central region of the aspheric surface as the fiducial sub-aperture. There are combinations of different amount of piston, tilt, power, astigmatism, coma and primary spherical between the misalignments of adjacent sub-apertures[16]. So each measurement needs to hold the following function for the correction of piston, tilt, power, astigmatism, coma and primary spherical:

$$\begin{aligned} w_0 &= w_1 + p_1 + a_1x_1 + b_1y_1 + c_1(x_1^2 + y_1^2) + d_1x_1y_1 \\ &+ e_1(x_1^2 - y_1^2) + f_1x_1(x_1^2 + y_1^2) + g_1y_1(x_1^2 + y_1^2) \\ &+ h_1(x_1^2 + y_1^2)^2 = w_2 + p_2 + a_2x_2 + b_2y_2 + c_2(x_2^2 + y_2^2) \\ &+ d_2x_2y_2 + e_2(x_2^2 - y_2^2) + f_2x_2(x_2^2 + y_2^2) + g_2y_2(x_2^2+y_2^2) \\ &+ h_2(x_2^2 + y_2^2)^2 \vdots = w_{M-1} + p_{M-1} + a_{M-1}x_{M-1}, \end{aligned} \tag{1}$$

where w_0 is the phase distribution of the fiducial subaperture, w_1,w_2, $\cdots$, w_{M-1} are the phase distributions of other subapertures, p_i, a_i, b_i, c_i are the coefficients of the relative translation errors to the fiducial subaperture of the displacement, tilt in the x and y directions and power respectively, d_i, e_i are the coefficients of the relative astigmatism, f_i, g_i are the coefficients of the relative coma, and h_i are the coefficients of the relative primary spherical.

By using least-squares fitting derived to minimize the sum of the squared differences in the all overlapping regions, as

$$\begin{aligned} S = &\sum_{j_1\neq 0}^{N_1}\sum_{i_1\subset W_0, W_{j_1}}^{n}\{W_0(x_{1i_1}, y_{1i_1}) - [W_{j_1}(x_{j_1i_1}, y_{j_1i_1}) \\ &+ p_{j_1}x_{j_1i_1} + a_{j_1}x_{j_1i_1} + b_{j_1}y_{j_1i_1} + c_{j_1}(x_{j_1i_1}^2 + y_{j_1i_1}^2) \\ &+ d_{j_1}x_{j_1i_1}y_{j_1i_1} + e_{j_1}(x_{j_1i_1}^2 - y_{j_1i_1}^2) + f_{j_1}x_{j_1i_1}(x_{j_1i_1}^2 + y_{j_1i_1}^2) \\ &+ g_{j_1}y_{j_1i_1}(x_{j_1i_1}^2 + y_{j_1i_1}^2) + h_{j_1}(x_{j_1i_1}^2 + y_{j_1i_1}^2)^2]\}^2 \\ &+ \sum_{j_2\cap j_3\neq 0}^{N_2}\sum_{i_2\subset W_{j_2}, W_{j_3}}^{n}\{[W_{j_2}(x_{j_2i_2}, y_{j_2i_2}) + p_{j_2}x_{j_2i_2} \\ &+ a_{j_2}x_{j_2i_2} + b_{j_2}y_{j_2i_2} + c_{j_2}(x_{j_2i_2}^2 + y_{j_2i_2}^2) + d_{j_2}x_{j_2i_2}y_{j_2i_2} \\ &+ e_{j_2}(x_{j_2i_2}^2 - y_{j_2i_2}^2) + f_{j_2}x_{j_2i_2}(x_{j_2i_2}^2 + y_{j_2i_2}^2) + g_{j_2}y_{j_2i_2} \\ &(x_{j_2i_2}^2 + y_{j_2i_2}^2) + h_{j_2}(x_{j_2i_2}^2 + y_{j_2i_2}^2)^2] - [W_{j_3}(x_{j_3i_2}, y_{j_3i_2}) \\ &+ p_{j_3}x_{j_3i_2} + a_{j_3}x_{j_3i_2} + b_{j_3}y_{j_3i_2} + c_{j_3}(x_{j_3i_2}^2 + y_{j_3i_2}^2) \\ &+ d_{j_3}x_{j_3i_2}y_{j_3i_2} + e_{j_3}(x_{j_3i_2}^2 - y_{j_3i_2}^2) + f_{j_3}x_{j_3i_2} \\ &(x_{j_3i_2}^2 + y_{j_3i_2}^2) + g_{j_3}y_{j_3i_2}(x_{j_3i_2}^2 + y_{j_3i_2}^2) \\ &+ h_{j_3}(x_{j_3i_2}^2 + y_{j_3i_2}^2)^2]\}^2 = \min, \end{aligned} \tag{2}$$

where W_0 is the phase distribution of the fiducial subaperture; (x_{1i_1}, y_{1i_1}), $(x_{j_1i_1}, y_{j_1i_1})$, $(x_{j_2i_2},\ y_{j_2i_2})$, $(x_{j_3i_2},\ y_{j_3i_2})$ denote the unified spatial coordinate system according to the reference sub-aperture; N_1 is the number of sub-apertures overlapping the fiducial; N_2 is the number of subapertures overlapping other subaperture excluding the fiducial one; n is the number of sampling points of each common region. The total number of the overlapping areas is $N_1 + N_2$.

Taking the differentiations of Eq. (2) with respect to these unknowns, the least squares equation can be de-

scribed as

$$\begin{cases} \frac{\partial S}{\partial p_i} = 0 \\ \frac{\partial S}{\partial a_i} = 0 \\ \frac{\partial S}{\partial b_i} = 0 \\ \frac{\partial S}{\partial c_i} = 0 \\ \frac{\partial S}{\partial d_i} = 0, \\ \frac{\partial S}{\partial e_i} = 0 \\ \frac{\partial S}{\partial f_i} = 0 \\ \frac{\partial S}{\partial g_i} = 0 \\ \frac{\partial S}{\partial h_i} = 0, \end{cases} \tag{3}$$

where i is an integer from 1 to $M-1$. Then the best splicing parameters can be found by solving the function, so the phase data of all the sub-apertures can be unified to the same benchmark.

After all the relative translation errors have been removed, we can obtain the accurate figure error of the full aperture.

We have tested a convex aspheric mirror to verify the proposed mathematical model and the stitching algorithm. The tested asphere with a clear aperture of 130 mm and a radius of curvature at the vertex of approximately 1 083.9 mm and the conic constant is –1.88. The experimental setup is shown in Fig. 3. There are a total of 6 dofs to align and null the interferometer or the subaperture. The Zygo interferometer is mounted on a y translation stage. The tested asphere is mounted on a three axes and x/z translation stage, which can be used to adjust the tip, tilt, defocus and the translation of x/z axis of the asphere precisely. The whole set up is mounted on a vibration isolator. We test the middle

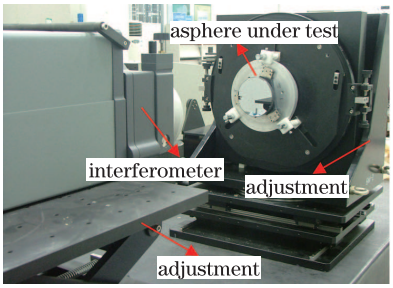

Fig. 3.(Color online) Setup of the stitching interferometry.

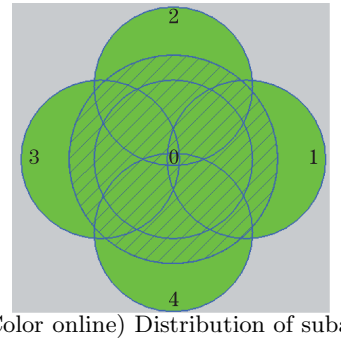

Fig. 4. (Color online) Distribution of subapertures.

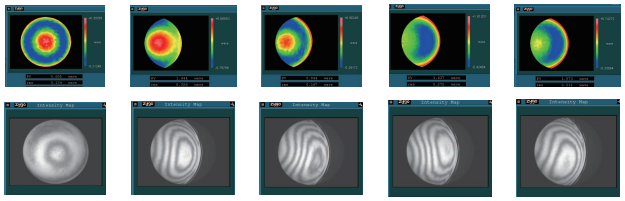

(a) middle subaperture (b) right subaperture (c) top subaperture (d) left subaperture (e) bottom subaperture

Fig. 5. (Color online) The corresponding interferograms and phase distributions of three subapertures.

sub-aperture firstly, and then translate the asphere in the x axis.

A lattice design that achieves coverage of the asphere with five subapertures is illustrated in Fig. 4, and the sub-aperture is about 75% of the full aperture. By aligning the interferometer and the tested asphere, adjusting the radius of the best-fitting sphere of each subaperture coincident with the focus of the transmission sphere, the test beam can retrace in the same way approximately, forming an interferogram between the reference beam and the test beam. The result of the five individual measurements is given in Fig. 5. Piston and tilt of each phase distribution have been removed.

Then all the sub-apertures can be unified into the same standard by homogeneous coordinate's transformation, and the translation error can be eliminated from each sub-aperture by using the indent simultaneous least-squares method. After all the translation errors have been removed, a final least-squares fitting is performed to evaluate the

Table 1 The Misalignment Coefficients by Least-squares Fitting

	x Tilt	y Tilt	Power
Coefficients	–0.0135745	0.0091536	–0.0052197

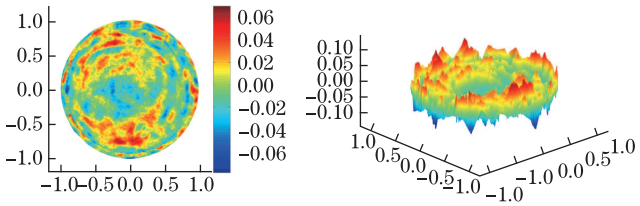

PV: 0.186 λ RMS: 0.019 λ

Fig. 6. (Color online) Normalized surface map of the whole aperture after stitching.

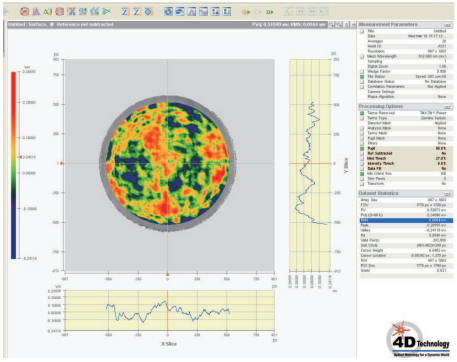

Fig. 7. (Color online) Phase map of the central field with the TMA system.

misalignment errors of the whole system. The misalignment coefficients are given in Table 1, where the tilt in the x and y directions, power and piston are –0.0021 833, –0.0135 745, 0.0091 536, and –0.0052 197, respectively.

We can obtain the exact figure error of the asphere by eliminating these errors. The surface map of the full aperture reconstructed by the stitching method is given in Fig. 6, where the peak-to-valley (PV) error is 0.186 λ and root-mean-square (RMS) error is 0.019 λ. Because of the random noise, there are slight systemic error and tiny misalignment errors between the adjacent sub-apertures and the stitched map is noisily shaped.

In order to validate the result, we have assembled the TMA system and measured the wavefront error of the central field by four-dimensional (4D) interferometer. The phase map of the central field is given in Fig. 7, where the PV and RMS are 0.346 and 0.068 λ, respectively. Noting that the TMA system approaches to diffraction limitation, the result concludes that SSI is feasible and accurate. Although only five sub-apertures were required to cover the full aperture in this experiment, the same stitching procedure can be extended to test those larger and deeper aspherical surfaces with more sub-apertures.

In conclusion, this letter utilizes the synthetical optimization stitching mode. The stitching algorithm is based on a simultaneous least-squares minimization method among all the overlapping regions which prevents the error from transmitting and accumulating. The physical concept of this method is clear. Data processing and mathematical operation are convenient. A convex asphere is measured with the method, and SSI is applied to the practical engineering. The results of the experiment conclude that this mathematical mode and stitching algorithm are feasible and effective. This technology has a wide scope of application. It can test large asphere, high numerical aperture asphere even for free-form surface. But the final accuracy depends on a series of factors including the precision of location of sub-apertures, the data acquisition and data reduction processes, the precision of wavefront reconstruction, and a variety of environmental efforts, which urge us to design the high-accuracy adjustment mechanism and improve the stitching algorithm continuously.

References

1. D. Malacara, *Optical Shop Testing* (John Wiley & Sons, New York, 1992).
2. H. Kutita, K. Saito, M. Kato, and T. Yatagai, Proc. SPIE **680,** 47(1987).
3. J. E. Negro, Appl. Opt. **23,** 1921 (1984).
4. M. Otsubo, O. K. Okada, and J. Tsujiuchi, Opt. Eng. **33,** 608 (1994).
5. J. Fleig, P. Dumas, P. E. Murphy, and G. W. Forbes, Proc. SPIE **5188,** 296 (2003).
6. A. Shorey, W. Kordonski, and M. Tricard, Proc. SPIE **5494,** 81 (2004).
7. C. J. Kim, Appl. Opt. **21,** 4521 (1982).
8. T. W. Stuhlinger, Proc. SPIE **656,** 118 (1986).
9. M. Otsubo, O. K. Okada, and J. Tsujiuchi, Proc. SPIE **1720,** 444 (1992).
10. M. Tricard, A. Shorey, B. Hallock, and P. Murphy, Proc. SPIE **6273,** 62730L (2006).
11. P. Murphy, J. Fleig, G. Forbes, D. Miladinovic, G. DeVries, and S. O'Dononue, Proc. SPIE **6293,** 62930J (2006).
12. M. Tricard, P. Dumas, and G. Forbes, Proc. SPIE **5638,** 284 (2005).
13. X. Wang, L. Wang, and X. Zhang, Opt. Precision Eng. (in Chinese) **15,** 192 (2007).
14. X. Wang and L. Wang, Chin. Opt. Lett. **5,** 645 (2007).
15. P. E. Murphy, J. Fleig, G. Forbes, and M. Tricard, Proc. SPIE **5786,** 112 (2005).
16. C. Zhao and J. H. Burge, Proc. SPIE **7063,** 706316 (2008).